Journal of Applied Biology & Biotechnology Vol. 14(6), pp. 119-126, November-December, 2026
Available online at http://www.jabonline.in
DOI: 10.7324/jabb.2026.316331

Multi-target modulation of prostate cancer signaling by *Boerhavia diffusa* leaf constituents: Insights from network pharmacology-guided *in silico* and *in vitro* approaches

Abeesha Jumana*, Junise Vazhayil, Swathi Harikumar, Afra Anas, Shafin Poonthiruthi, Rabin M. Jafar
Department of Pharmaceutics, Al Shifa College of Pharmacy, Affiliated to KUHS, Perinthalmanna, Malappuram, India.

ARTICLE INFO

Article history:
Received on: 04/04/2026
Accepted on: 09/07/2026
Available Online: 25/09/2026

Key words:
Boerhavia diffusa, Network pharmacology, Prostate cancer, Molecular docking

ABSTRACT

Prostate cancer (PC) remains a leading cause of male cancer mortality, and current treatments are frequently constrained by resistance, toxicity, and cost. *Boerhavia diffusa* (Punarnava) is widely used in traditional medicine, but its precise molecular mechanisms in PC are not well defined. This study integrated LC/MS-based phytochemical profiling, network pharmacology, molecular docking, and *in vitro* cytotoxicity to clarify the multi-target anticancer potential of *B. diffusa* leaf. LC/MS of the ethanolic extract tentatively identified eight major constituents; perakine and canavalioside were prioritized for systems analysis based on drug-likeness. Predicted targets (SwissTargetPrediction) were merged with PC genes (GeneCards) to generate a STRING-Cytoscape interaction network, revealing 10 hub nodes [epidermal growth factor receptor (EGFR), signal transducer and activator of transcription 3, caspase 3, AKT serine/threonine kinase 1 (AKT1), heat shock protein 90 alpha family class A member 1, catenin beta 1, BCL-2-like protein 1, SRC, insulin-like growth factor 1 receptor, and matrix metalloproteinase 2] enriched in PI3K-Akt, EGFR, and matrix-remodeling pathways. Docking showed that canavalioside binds AKT1 more strongly than perakine, while perakine exhibits a slightly more favorable docking score for PI3Kα; together, the two ligands form dense hydrogen-bond networks within functionally relevant regions of the PI3K-Akt axis. Consistently, the ethanolic *B. diffusa* leaf extract reduced PC-3 cell viability in a concentration-dependent manner with an IC_{50} of 57.213 µg/ml, providing preliminary functional support for the predicted multi-target antiproliferative activity.

1. INTRODUCTION

Prostate cancer (PC) continues to be one of the most common causes of cancer-associated morbidity and mortality in men worldwide, and existing treatments are often hampered by resistance, toxicity, and higher cost [1]. This has been overcome by herb-derived scaffolds that are able to modulate several cancer pathways at the same time [2,3]. The ethnomedicinal herb *Boerhavia diffusa* (BDA) (Punarnava), commonly used in Indian traditional practice, has been reported to possess pharmacological activities such as antioxidant, anti-inflammatory, and cytoprotective effects [4,5]; however, the molecular mechanisms of BDA in PC are not well defined.

Network pharmacology (NPY) provides a systems-level approach to decode how a complex phytochemical compound affects interconnected signaling networks instead of individual targets [6,7]. With the addition of molecular docking and *in vitro* assessment, this approach can bridge the gap between empirical phytochemical use and mechanism-based drug discovery [8–10]. The present study employed LC/MS profiling of BDA leaf extract to tentatively identify major therapeutic phytoconstituents and systematic evaluation of PC related genes and construction of a compound target pathway network. Hub proteins in PI3K/Akt and related signaling axes were prioritized as putative drivers of the observed pharmacological characteristics. Experimental studies in prostate cancer models have implicated PI3K/Akt/mTOR signaling in tumor-cell migration, invasion, autophagy, and apoptosis [11,12].

The PI3K/AKT signaling cascade is a major pathway involved in the progression of PC [13]. PI3K activation produces PIP3, which recruits and activates AKT serine/threonine kinase 1 (AKT1) at the plasma membrane, stimulating cell survival, proliferation, metabolism, and resistance to treatment. The loss of PTEN and overexpression of PI3K activate AKT1 in PC, and this is associated with higher-grade disease, biochemical recurrence, and castration-resistant phenotypes [14]. In PC models, experimental inhibition of PI3K/AKT signaling reduces cell proliferation, induces apoptosis, and sensitizes cells to other treatments, further highlighting AKT1

*Corresponding Author
Abeesha Jumana, Department of Pharmaceutics, Al Shifa College of Pharmacy, Affiliated to KUHS, Perinthalmanna, Malappuram, India.
E-mail: abeeshaajas05 @ gmail.com

and PI3K as potential therapeutic targets and rational targets for docking and NPY [11–13].

The present research work lies in integrating LC/MS-guided putative phytochemical characterization, NPY, and structure-based molecular docking specifically focused on PC, rather than on generic antioxidant or anti-inflammatory endpoints commonly reported for BDA. Detailed molecular docking against AKT1/PI3K proteins provides structural insight into how these ligands might stabilize inhibitory conformations of survival signaling proteins, and these *in silico* predictions are preliminarily supported by MTT-based antiproliferative activity in PC-3 cells, without directly demonstrating specific pathway modulation. This triangulation of LC/MS data, network-level analysis, docking, and *in vitro* evaluation positions BDA leaf metabolites as promising scaffolds for rational optimization against PC and illustrates a transferable workflow for deconvoluting other ethnomedicinal herbs.

2. MATERIALS AND METHODS

2.1. Collection, identification, and extraction of raw material

The plant Punarnava (*Boerhavia diffusa* L.) was collected from Manjeri, Malappuram, Kerala and authenticated by a botanist at MES Kalladi College, Mannarkkad, Palakkad. The foreign matter, earthy matter, and leaf residue were thoroughly washed off and extracted after shade drying. A quantity of 150 g of powdered, dried leaves was placed in a Soxhlet apparatus and exhaustively extracted with 500 ml of ethanol for 48 hours (at 50°C). The plant extract was concentrated by solvent evaporation to dryness, and the crude extract was transferred to a pre-dried borosil desiccator (Flange model-3082041) until constant weight was achieved, and the residual moisture was removed. The dried extract was weighed, and the percentage yield was determined on the basis of the original plant material with a mean yield of 12.23% ± 1.43%. The final leaf extract was stored at 4°C in an airtight container for phytochemical and biological evaluations.

2.2. LC/MS analysis

From the ethanolic leaf extract of *B. diffusa* (ELBD), phytoconstituents were preliminarily identified, and the putative constituents were characterized in detail using the quadrupole time-of-flight (Q-TOF) LC/MS [15]. The analyses were done on a Mariner Biospectrometry Q-TOF system that was equipped with a binary pump and coupled to an Agilent 1260 Infinity I HPLC fitted with an electrospray ionization source that operated in negative full-scan mode (m/z 100–1200) at a source temperature of 140°C. Chromatographic separation was employed by a Phenomenex Luna C8 column (150 × 2 mm, 5 µm), providing reversed-phase resolution of moderate to strong hydrophobic metabolites. Ethanol containing 0.3% formic acid was used as the mobile phase and delivered isocratically at 0.1 ml/minute, with the eluent directed online to the ESI interface [15,16]. Putative metabolite identities were supported by high-resolution accurate mass measurements and isotopic patterns, which were compared with published data and spectral libraries.

2.3. Target identification, pathway enrichment analysis, gene ontology, and network construction

LC/MS tentatively identified phytochemicals from ELBD were first matched with PubChem to obtain standardized 2D/3D structures suitable for computational analysis. The putative human protein targets of each compound were predicted using SwissTargetPrediction [17], and PC-related genes were retrieved from GeneCards [18]. Their intersection was determined using Venny 2.1 to yield common candidate genes. These overlapping targets were imported into the STRING database to construct a protein–protein interaction network, which was visualized and topologically analyzed in Cytoscape to identify key nodes and subnetworks [19,20]. Subsequently, ShinyGO [21] and the DAVID platform [22] were used to perform Gene Ontology and pathway enrichment analyses for the intersecting genes. SRplot was used to generate graphical summaries of significantly enriched pathways and core targets to guide the selection of representative proteins for molecular docking.

2.4. Molecular interaction study

For docking, two PI3K/Akt pathway proteins relevant to PC, AKT1 (PDB 4EKL), and PI3K (PDB 4OVV) were retrieved as X-ray structures from the RCSB PDB. For PI3Kα, PDB ID: 4OVV, docking was performed on the p110α catalytic subunit (chain A), the Glide receptor grid was centered at coordinates (32.1, 18.4, 54.7) Å with a cubic box of (20.0 × 20.0 × 20.0) Å, and the residue numbering and chain identity were cross-checked against UniProt and RCSB PDB records to ensure that residues from the C2 domain were not mis-annotated as catalytic-site residues. These proteins were selected because PI3K/AKT signaling plays a crucial role in regulating survival, metabolism, proliferation and angiogenesis in PC [11,13]. Corresponding ligand 2D structures were downloaded from PubChem and prepared for docking. Each protein was refined in the Schrödinger Protein Preparation Wizard with Epik, including protonation-state assignment, hydrogen-bond optimization, rebuilding of missing side chains or loops using Prime, addition of heteroatoms, and restrained minimization. Glide receptor grids (20Å cubic box) were generated around the known or predicted active sites, and docking simulations and scoring were performed in Glide via the Maestro interface. The binding region of each protein was further adjusted to allow ligand placement within 5 Å of the active-site center [23–26].

2.5. *In vitro* anticancer study

Viable PC-3 PC cells (procured from the cell repository of the National Centre for Cell Sciences, Pune, India), Dulbecco's Modified Eagle Medium, were used to maintain the cell line, supplemented with 10% Fetal Bovine Serum. Penicillin (100 U/ml) and streptomycin (100 µg/ml) were added to the medium to prevent bacterial contamination, maintained in a humidified environment with 5% CO_2 at 37°C. The cells were seeded at 1 × 104 cells/well in 96-well plates and allowed to adhere for 24 hours before treatment. Cells were then treated with ELBD at 10, 20, 40, 60, 80, and 100 µg/ml concentrations for 24 hours at 37°C, and each concentration was tested in triplicate wells in at least three independent experiments. Control wells received medium containing the vehicle [0.1% dimethyl sulfoxide (DMSO)] only [9]. After 24 hours of exposure to ELBD, 20 µl of MTT stock solution (5 mg/ml in PBS) was added to each well to achieve a final MTT concentration of 0.5 mg/ml, and plates were incubated for 4 hours at 37°C to allow formazan crystal formation. 100 µl of concentrated DMSO was used to dissolve the purple formazan precipitate. The vitality of the cells was determined by measuring the absorbance at 540 nm using a multi-well plate reader. Data were expressed as the percentage of viable cells relative to the vehicle-treated control [27,28]. The cell viability was normalized to the vehicle control, and the percentage inhibition of cell growth was calculated according to the formula,

$$\% \text{ inhibition} = [\frac{(A_{control} - A_{sample})}{A_{control}}] \times 100$$

Where A is the absorbance.

2.6. Statistical analysis

The network study has set $p < 0.05$ to select the target genes. Molecular interaction study was performed multiple times to generate an exact docking score. The *in vitro* data were expressed as mean ± SEM of at least three independent experiments. IC_{50} values and the dose-response curves were generated in GraphPad Prism (version 9). Statistical comparisons between groups were performed using one-way ANOVA followed by Tukey's post hoc test, with $p < 0.05$ considered significant.

3. RESULTS AND DISCUSSION

3.1. Phytoconstituent analysis

After preliminary phytochemical investigation, LC/MS profiling of ELBD revealed eight major putatively annotated phytoconstituents, including gravacridonetriol, purpurin, perakine, dipiperamide C, canavalioside, eucommin A, kukoamine D, and the triterpenoid avenestergenin A2 (Table 1).

Gravacridonetriol and dipiperamide C, among the putatively identified bioactive metabolites of ELBD, are alkaloids with aromatic and amide-type properties. Canavalioside and eucommin A are glycosidic metabolites. Kukoamine D is a polyamine-containing phenolic derivative, while avenestergenin A2 is a triterpenoid. These chemotypes contribute to the polypharmacology with potential antioxidant and anticancer properties of ELBD. Purpurin, which is a naturally occurring hydroxylated anthraquinone, has been a subject of interest because of its anticancer property [29]. One study showed that the compound may inhibit cancer growth, induce apoptosis, and affect many cancer pathways, making the compound a bioactive molecule and suggesting it could be used to develop safer and more effective anticancer therapies. The piperamide alkaloid has demonstrated promising anticancer effects, notably by inhibiting tumor cells that are resistant to multiple drugs [30]. This suggests that these alkaloids could potentially serve as promising lead compounds for future cancer therapies. Research interest has been directed toward Avenestergenin A2 due to its potential anticancer activity, its ability to target metabolic pathways linked to cancer and inhibit abnormal cellular proliferation. The coexistence of these complementary scaffolds suggests that the ELBD may exert anticancer effects and support the ethnomedicinal application of BDA in tumor conditions. Based on drug-likeness criteria and predicted engagement of cancer-relevant protein families, perakine and canavalioside were prioritized as representative ligands for downstream NPY and docking analyses. Figure 1 represents the LC/MS chromatogram of perakine and canavalioside from BDA leaf.

3.2. Prediction of potential molecular targets

Perakine and canavalioside, tentatively identified from the ELBD, were prioritized for in-depth systems analysis because they met standard drug-likeness criteria and displayed broad predicted engagement of cancer-relevant protein families, including kinases and apoptosis regulators, in SwissTargetPrediction, to infer plausible human protein targets based on ligand similarity principles [17]. The resulting target profiles (200 targets for two active compounds) indicated that Perakine and canavalioside engage diverse protein families including kinases, apoptosis regulators, and membrane receptors, suggesting broad regulatory potential relevant to PC biology. SwissTargetPrediction was queried in "Homo sapiens" mode and predicted targets with non-zero probability, collected and curated to retain high-confidence interactions relevant to cancer biology [17]. Several predicted targets were functionally linked to cell proliferation, survival signaling and metastatic behavior, implying that these phytoconstituents may modulate multiple oncogenic nodes rather than a single pathway. This multi-target pattern supports the suitability of an NPY framework for understanding the anticancer evaluation of BDA leaf constituents.

3.3. Gene collection and target identification

Genes prioritized from the GeneCards database had high integration scores across genomic, transcriptomic, and clinical annotations, in which the enriched molecules were highly implicated in tumor initiation, progression, or therapy resistance, such as oncogenes, tumor suppressors, signaling adaptors, and extracellular matrix modulators [31–33], creating a disease network scaffold. These curated PC genes along with compound-derived targets were used for overlap analysis to ensure that downstream network construction focused on biologically relevant intersections between BDA ligands and known drivers of PC. Genes with high GeneCards relevant scores for PC were selected to build a disease-associated set, and overlap between this set and compound-derived targets was determined using Venny 2.1 to define shared nodes for subsequent network construction.

Table 1. Major putatively annotated phytochemicals from *Boerhavia diffusa* leaf by LC/MS analysis in negative ESI mode.

Sl No.	Compound name	Molecular formula	Neutral mass	Ion/adduct used for assignment	Measured m/z (Q TOF)	Mass error* (ppm)	Retention time (minute)
1.	Gravacridonetriol	$C_{19}H_{19}NO_6$	357.121,239	$[M-H]^-$	357.1216	+1.01	1.054
2.	Purpurin	$C_{14}H_8O_5$	256.037,175	$[M-H]^-$	256.0369	−1.07	3.249
3.	Perakine	$C_{21}H_{22}N_2O_3$	350.163,043	$[M-H]^-$	350.1630	−0.12	6.534
4.	Dipiperamide C	$C_{33}H_{36}N_2O_6$	556.257338	$[M-H]^-$	556.2574	+0.11	8.990
5.	Canavalioside	$C_{26}H_{42}O_{12}$	546.267,630	$[M-H]^-$ / $[M+HCOO]^-$	546.2688	+2.14	9.775
6.	Eucommin A	$C_{27}H_{34}O_{12}$	550.205,030	$[M-H]^-$ / $[M+HCOO]^-$	550.2057	+1.22	6.852
7.	Kukoamine D	$C_{28}H_{42}N_4O_6$	530.310,436	$[M-H]^-$	530.3121	+3.14	12.453
8.	Avenestergenin A2	$C_{37}H_{52}O_7$	608.371,305	$[M-H]^-$	608.3701	−1.98	15.970

* Mass error values were calculated relative to the neutral monoisotopic mass derived from the molecular formula.

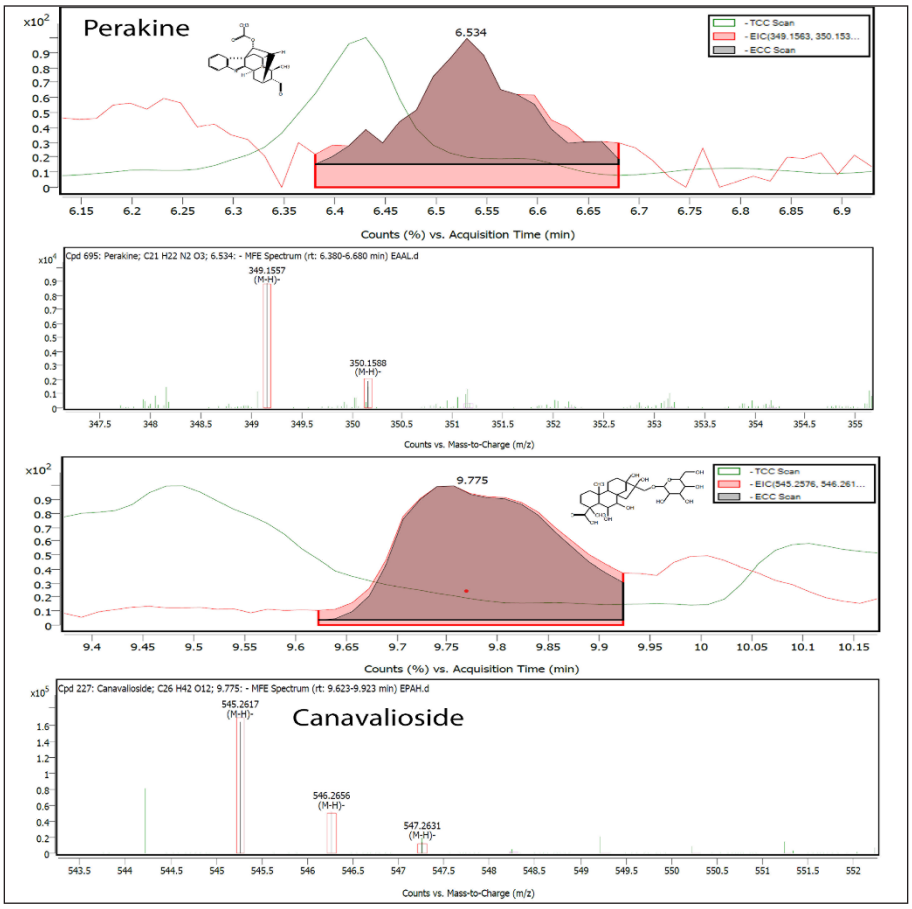

Figure 1. LC/MS chromatogram of perakine and canavalioside from *Boerhavia diffusa* leaf.

3.4. Protein–protein interaction and network construction

Common targets from the Venny analysis were uploaded to STRING to construct a protein–protein interaction network using a confidence threshold above 0.4, thereby excluding poorly supported connections (Fig. 2). The resulting network displayed dense connectivity among several nodes that indicates many overlapping targets participate in shared signaling axes rather than functioning in isolation [34,35]. Clusters within the network corresponded to pathways linked with growth factor signaling, apoptosis regulation, and cytoskeletal remodeling, all central to PC biology. This interactome provided a structural basis for identifying hub proteins with high degree and betweenness, which may serve as key leverage points for modulation by BDA-derived ligands.

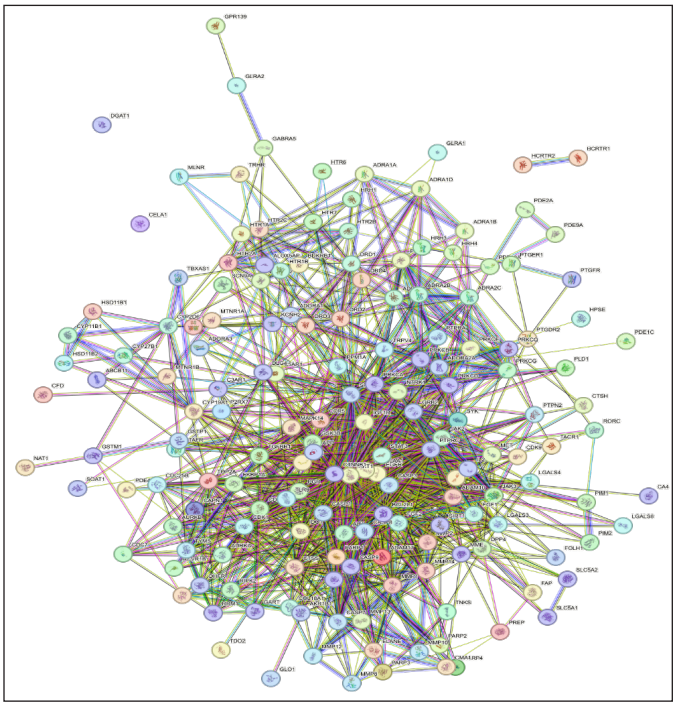

Figure 2. The protein–protein interaction for the hub genes using the STRING database.

3.5. Topological analysis

The STRING-derived interaction file was imported into Cytoscape for detailed topological evaluation of overlapping targets [35,36]. Network metrics such as degree, closeness and betweenness centrality were applied to rank nodes, yielding ten prominent hub genes, epidermal growth factor receptor (EGFR), signal transducer and activator of transcription 3, caspase 3, AKT serine/threonine kinase 1 (AKT1), heat shock protein 90 alpha family class A member 1, catenin beta 1, BCL-2-like protein 1, SRC, insulin-like growth factor 1 receptor, and matrix metalloproteinase 2. In Cytoscape, degree, closeness, and betweenness centrality were computed using standard network analysis plugins, and

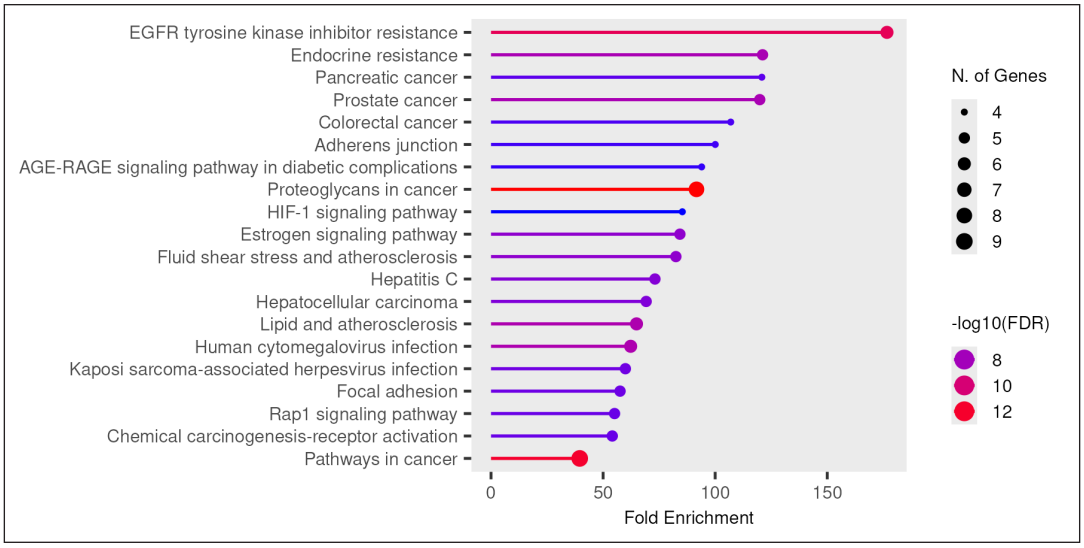

Figure 3. KEGG pathway fold enrichment analysis using ShinyGO 0.85.1, showing correlation between ligands and the top 10 types of prostate cancer pathways. The horizontal axis represents the fold enrichment score, and the vertical axis shows different types of pathways associated with cancer.

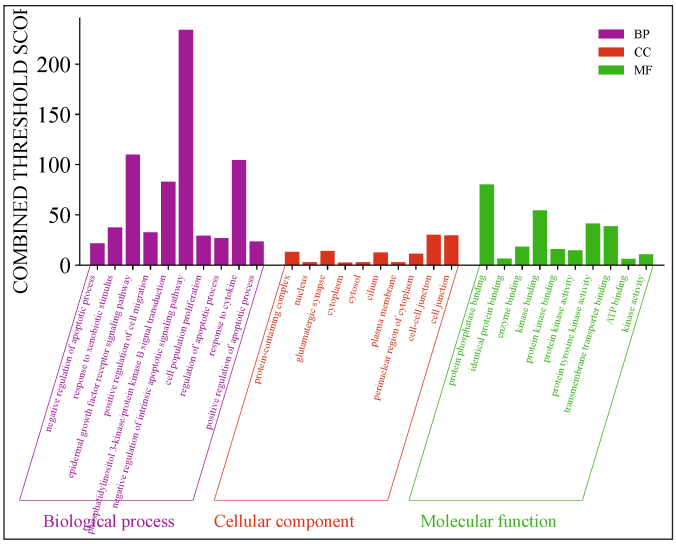

Figure 4. Annotation information for the ligands based on DAVID and SRplot analyses. Top enriched Gene Ontology terms for intersecting/common target genes at p-value < 0.05.

nodes with high centrality values were highlighted as hub proteins in the visualized interactome, facilitating identification of key regulatory cores for docking. These hubs are integral regulators of proliferation, survival, invasion and treatment resistance in PC, indicating that phytoconstituents may collectively influence multiple hallmarks of malignancy. Visualization in Cytoscape highlighted these genes as densely connected cores within the network, reinforcing their importance as candidate molecular targets for subsequent docking and mechanistic validation.

3.6. Functional enrichment analysis

Common targets were subjected to Gene Ontology and KEGG pathway enrichment using the DAVID platform [22], applying a significance threshold of p < 0.05 or adjusted FDR (Fig. 3). Biological process terms were enriched for regulation of apoptosis, cell proliferation, inflammatory response, and signal transduction, whereas molecular function categories involved protein kinase activity, growth factor binding, and enzyme regulation. Cellular component results indicated localization to the plasma membrane, cytosol and nucleus, consistent with signaling hubs. KEGG analysis highlighted pathways such as PI3K-Akt, EGFR-related signaling, and extracellular matrix remodeling, collectively suggesting that BDA ligands may modulate interconnected oncogenic circuits rather than a single linear cascade in PC. Figure 4 represents the annotation information of ligands by the DAVID database and SRplot tool.

3.7. Molecular interaction study

Docking analysis revealed that canavalioside showed the most favorable binding toward AKT1, with a markedly lower docking score against 4EKL (−12.711 kcal/mol) compared to perakine (−8.312 kcal/mol), whereas perakine exhibited slightly more favorable docking score for PI3Kα (4OVV; −7.416 *vs.* −6.888 kcal/mol), indicating complementary engagement of the PI3K-Akt axis by these two ligands (Fig. 5). Canavalioside formed multiple stabilizing hydrogen bonds with key active-site residues in 4EKL (GLU234, ASP439, LEU156, TYR437, GLU278, and THR160) and engaged GLU468, GLU469, ARG472, and ARG461 within the C2 domain of PI3Kα protein (4OVV), indicating a dense interaction network in the membrane-associated region while docking grids were centered on the catalytic domain. Thus, the analysis distinguishes interactions of canavalioside with the ATP-binding/catalytic pocket of the p110α subunit (chain A) and its additional contacts with C2-domain residues (GLU468, GLU469, ARG472, and ARG461), which lie outside the catalytic site but were retained as membrane-associated contacts in the 2D interaction diagram for completeness. Perakine showed fewer polar contacts, limited mainly to LYS276 in 4EKL and ARG472/GLU468 in 4OVV, and lacked notable hydrophobic contacts, consistent with its weaker overall binding. The presence of both extensive hydrogen bonding and hydrophobic anchoring at GLN79 in 4EKL for canavalioside suggests that this glycosidic ligand may more effectively stabilize inhibitory poses at AKT1, supporting its

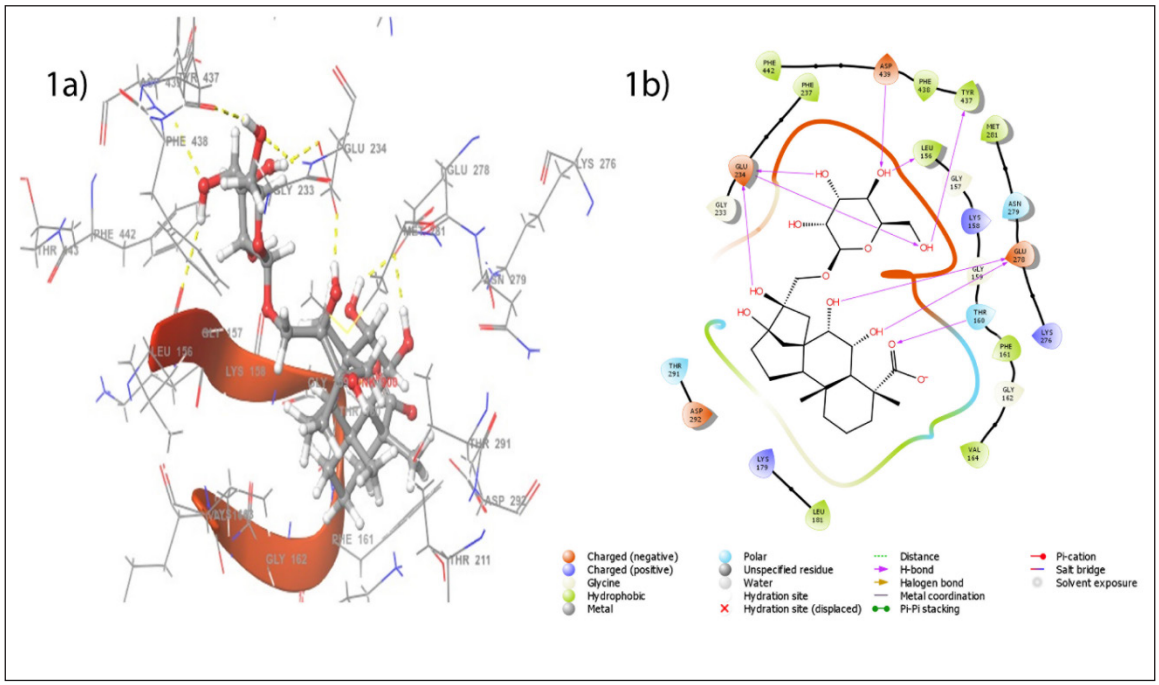

Figure 5. Molecular interaction diagram (3D and 2D) of canavalioside with AKT serine/threonine kinase 1 protein (docking score:−12.711 kcal/mol).

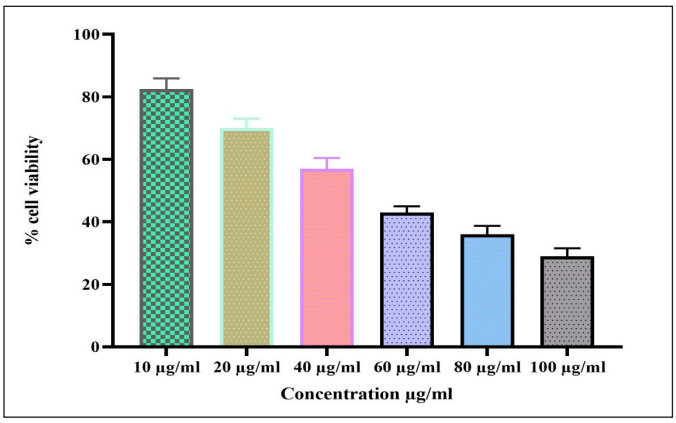

Figure 6. In the MTT assay, the PC-3 cells were exposed to the ethanolic leaf extract of *B. diffusa* for 24 hours. The data are expressed as mean ± SEM, with IC_{50} = 57.213 µg/ml.

designation as a principal contributor to the predicted anti-PC activity of *B. diffusa* alongside perakine.

3.8. *In vitro* anticancer activity

Treatment of PC-3 cells with ELBD produced a clear concentration-dependent reduction in cell viability. The cell survival was decreased from 82.43% at 10 µg/ml to 29.25% at 100 µg/ml, corresponding to an increase in growth inhibition from 17.57% to 70.75%. Nonlinear regression of the dose–response curve yielded an IC_{50} value of 57.213 µg/ml, indicating moderate cytotoxic potency of ELBD against PC3 cells (Fig. 6).

The progressive loss of cell viability with increasing concentrations may suggest that ELBD exerts a direct cytotoxic or growth-inhibitory effect on androgen-independent PC-3 cells (IC_{50} = 57.213 µg/ml). These findings align with the NPY prediction for the BDA ligands to target key survival signaling nodes such as AKT1 and PI3K, supporting their potential to interfere with proliferation and promote cell death in PC. As the data were derived from a single PC cell line (PC-3) using one viability assay, they should be interpreted as preliminary evidence of antiproliferative activity rather than definitive proof of a specific signaling mechanism. Future studies will extend with additional PC models and nonmalignant prostate epithelial cells, and will incorporate apoptosis, ROS and targetspecific readouts to validate and refine the proposed network-level mechanisms.

4. CONCLUSION

This study systematically explored the multi-target modulation of PC signaling by ELBD constituents through an integrated workflow combining LC/MS-based metabolite profiling, NPY-guided target and pathway analysis, structure-based docking and MTT-based *in vitro* cytotoxicity in PC-3 cells. Perakine and canavalioside emerged as key ligands targeting central nodes within the PI3K/Akt axis and related signaling hubs, with canavalioside showing stronger binding to AKT1 and perakine displaying a slightly more favorable docking score for PI3Kα, thereby providing a complementary mechanistic framework for the putative anticancer actions of ELBD. The enriched pathways and hub genes identified suggest that ELBD may exert multi-target modulation of proliferation, survival and microenvironment-related processes, representing a predicted network-level mechanism rather than an experimentally proven signaling pathway. Consistent with the NPY and docking predictions, ELBD produced a concentration-dependent reduction in PC3 cell viability (IC_{50} = 57.213 µg/ml), indicating moderate antiproliferative activity in this preliminary *in vitro* model. However, because this study was based on a single cell line and an MTT readout, the proposed AKT1/PI3K-mediated mechanism remains putative and will require further mechanistic and comparative *in vitro* studies for confirmation.

5. AUTHORS' CONTRIBUTIONS

All authors played an active role in the planning of the study and in the collection, analysis, or interpretation of the data. Each author also contributed to writing the manuscript or critically revising it for important intellectual content. All authors reviewed and approved the final version for submission and agree to be accountable for the accuracy and integrity of the work. They also accept responsibility for addressing any questions related to the study. In addition, all authors satisfy the authorship requirements of the International Committee of Medical Journal Editors (ICMJE).

6. FUNDING

There was no funding for this study.

7. CONFLICTS OF INTEREST

The authors report no financial or any other conflicts of interest in this work.

8. ETHICAL APPROVAL

This research did not involve any experiments related to animals or humans.

9. DATA AVAILABILITY

All data are accessible from the authors and will be provided upon request.

10. PUBLISHER'S NOTE

All assertions made in this article are exclusively those of the writers and do not necessarily reflect the views of the publisher, editors, or reviewers. This journal maintains neutrality about jurisdictional claims related to reported institutional affiliations.

11. USE OF ARTIFICIAL INTELLIGENCE (AI)-ASSISTED TECHNOLOGY

The authors declare that an AI-assisted tool (Grammarly, San Francisco, USA) was used during manuscript preparation solely for English-language enhancement, grammatical correction, and reference formatting. No AI-assisted tool was used for the generation of scientific content, experimental data, research concepts, analysis, or interpretation of results. All edits suggested by the AI tool were carefully reviewed, verified, and approved by the authors prior to submission. The authors assume full responsibility for the accuracy and integrity of the content presented in this work.

REFERENCES

1. Culp MB, Soerjomataram I, Efstathiou JA, Bray F, Jemal A. Recent global patterns in prostate cancer incidence and mortality rates. Eur Urol 2020;77(1):38–52; doi: https://doi.org/10.1016/j.eururo.2019.08.005
2. Siddiqui AJ, Adnan M, Saxena J, Alam MJ, Abdelgadir A, Badraoui R, *et al.* Therapeutic potential of plant-and marine-derived bioactive compounds in prostate cancer: mechanistic insights and translational applications. Pharmaceuticals 2025;18(3):286; doi: https://doi.org/10.3390/ph18030286
3. Suhail P, Venkatachalam VV, Balasubramanian T, Murali R, Renganathan AB. Evaluation of anticancer activity of *Annona muricata* leaf targeting FGFR3 and EGFR receptors against bladder and lung cancer. J Appl Pharm Sci 2025;15(4):95–101; doi: https://doi.org/10.7324/JAPS.2025.224656
4. Yadav A. *Boerhavia diffusa* L.(Punarnava): a comprehensive review on ethnobotany, phytochemistry, pharmacology, and therapeutic applications. Int J Pharm Sci Med 2024;2:145–51; doi: https://doi.org/10.70199/IJPSM.2.4.145-151
5. Dora BB, Gupta S, Sital S, Pastore A. Punarnava (*Boerhavia diffusa*): a promising indigenous herbal drug and its effect on different disease conditions. Res Rev J Herbal Sci 2018;4(2):21–4; doi: https://doi.org/10.37591/rrjohs.v4i2.715
6. Mukherjee PK, Banerjee S, Kar A. Molecular combination networks in medicinal plants: understanding synergy by network pharmacology in Indian traditional medicine. Phytochem Rev 2021;20(4):693–703; doi: https://doi.org/10.1007/s11101-020-09730-4
7. Gertsch J. Botanical drugs, synergy, and network pharmacology: forth and back to intelligent mixtures. Planta Med 2011;77(11):1086–98; doi: https://doi.org/10.1055/s-0030-1270904
8. Mir WR, Bhat BA, Kumar A, Dhiman R, Alkhanani M, Almilaibary A, *et al.* Network pharmacology combined with molecular docking and *in vitro* verification reveals the therapeutic potential of Delphinium roylei munz constituents on breast carcinoma. Front Pharmacol 2023;14:1135898; doi: https://doi.org/10.3389/fphar.2023.1135898
9. Suhail P, Venkatachalam VV, Joseph S, Murali R, Renganathan AB. *In vitro* Anticancer potential and Molecular modelling study of Flavanol Glucoside from Graviola (*Annona muricata*) fruit: a potential inhibitor of antiapoptotic proteins. Lett Appl NanoBioSci 2024;13(4):167; doi: https://doi.org/10.33263/LIANBS134.167
10. Rebeea VM, Muhsina A, Rameesa M, Fathima HS, Shanibah T, Ashik T, *et al.* Identification of phytochemicals and evaluation of anticancer activity of peels of *Carica papaya* fruit. J Res Pharm 2025;29(5):2143–50; doi: https://doi.org/10.12991/jrespharm.1766388
11. Vo BT, Morton Jr D, Komaragiri S, Millena AC, Leath C, Khan SA. TGF-β effects on prostate cancer cell migration and invasion are mediated by PGE2 through activation of PI3K/AKT/mTOR pathway. Endocrinology 2013;154(5):1768–79; doi: https://doi.org/10.1210/en.2012-2074
12. Kumar D, Shankar S, Srivastava RK. Rottlerin induces autophagy and apoptosis in prostate cancer stem cells via PI3K/Akt/mTOR signaling pathway. Cancer Letters 2014;343(2):179–89; doi: https://doi.org/10.1016/j.canlet.2013.10.003
13. Wang R, Qu Z, Lv Y, Yao L, Qian Y, Zhang X, *et al.* Important roles of PI3K/AKT signaling pathway and relevant inhibitors in prostate cancer progression. Cancer Med 2024;13(21):e70354; doi: https://doi.org/10.1002/cam4.70354
14. Shorning BY, Dass MS, Smalley MJ, Pearson HB. The PI3K-AKT-mTOR pathway and prostate cancer: at the crossroads of AR, MAPK, and WNT signaling. Int J Mol Sci 2020; 21(12):4507; doi: https://doi.org/10.3390/ijms21124507
15. Xie C, Zhong D, Yu K, Chen X. Recent advances in metabolite identification and quantitative bioanalysis by LC–Q-TOF MS. Bioanalysis 2012;4(8):937–59; doi: https://doi.org/10.4155/bio.12.43
16. Samy S, Robinson J, Hays MD. An advanced LC-MS (Q-TOF) technique for the detection of amino acids in atmospheric aerosols. Anal Bioanal Chem 2011;401(10):3103–13; doi: https://doi.org/10.1007/s00216-011-5238-2
17. Daina A, Michielin O, Zoete V. SwissTargetPrediction: updated data and new features for efficient prediction of protein targets of small molecules. Nucleic Acids Res 2019;47(1):W357–64; doi: https://doi.org/10.1093/nar/gkz382
18. Stelzer G, Rosen N, Plaschkes I, Zimmerman S, Twik M, Fishilevich S, *et al.* The GeneCards suite: from gene data mining to disease genome sequence analyses. Curr Protocols Bioinf 2016;54(1):1–30; doi: https://doi.org/10.1002/cpbi.5
19. Szklarczyk D, Gable AL, Nastou KC, Lyon D, Kirsch R, Pyysalo S, *et al.* The STRING database in 2021: customizable protein–protein networks, and functional characterization of user-uploaded gene/measurement sets. Nucleic Acids Res 2021;49(D1):D605–12; doi: https://doi.org/10.1093/nar/gkaa1074

20. Shannon P, Markiel A, Ozier O, Baliga NS, Wang JT, Ramage D, *et al.* Cytoscape: a software environment for integrated models of biomolecular interaction networks. Genome Res 2003;13(11):2498–504.
21. Ge SX, Jung D, Yao R. ShinyGO: a graphical gene-set enrichment tool for animals and plants. Bioinformatics 2020;36(8):2628–9; doi: https://doi.org/10.1093/bioinformatics/btz931
22. Sherman BT, Hao M, Qiu J, Jiao X, Baseler MW, Lane HC, *et al.* DAVID: a web server for functional enrichment analysis and functional annotation of gene lists (2021 update). Nucleic Acids Res 2022;50(W1):W216–W21; doi: https://doi.org/10.1093/nar/gkac194
23. Schrödinger, Inc. Schrödinger: computational platform for molecular discovery and design [Internet]. New York (NY): Schrödinger, Inc.; c1990–2026. Available via https://www.schrodinger.com/ (Accessed 01 April 2025).
24. Dinesh Adottu D, Mankulathil Shajahan A, Koolaparambil SA, Rasheed SP, Vengamthodi A, Pattilthodika S, *et al.* Investigating the activity of Quinazoline derivatives against T790 mutant EGFR receptors employing computer-aided drug design. J Appl Pharm Sci 2024;14(9):69–75; doi: https://doi.org/10.7324/JAPS.2024.188300
25. Suhail P, Ashwini HV, Asna K, Bagyasree K, Thirupathi AT, Joy J. Phytochemical screening and anticancer profiling of *Artocarpus altilis* (Breadfruit) leaves against colorectal cancer. J Res Pharm 2026;30(1):94–105; doi: https://doi.org/10.12991/jrespharm.1658438
26. Vallikkaparambil M, Kalakkandan H, Koomankottil MS, Shareef S, Nishida M, Joy J, *et al.* Phytochemical Screening and Anticancer Evaluation of Ethanolic Root Extract of Asparagus gonoclados Baker: insight for Colorectal Cancer Treatment. Tradit Integr Med 2026;11(1):15–25; doi: https://doi.org/10.18502/tim.v11i1.21240
27. Mokhtari MJ, Motamed N, Shokrgozar MA. Evaluation of silibinin on the viability, migration and adhesion of the human prostate adenocarcinoma (PC-3) cell line. Cell Biol Int 2008;32(8):888–92; doi: https://doi.org/10.1016/j.cellbi.2008.03.019
28. Kamalidehghan B, Ghafouri-Fard S, Motevaseli E, Ahmadipour F. Inhibition of human prostate cancer (PC-3) cells and targeting of PC-3-derived prostate cancer stem cells with koenimbin, a natural dietary compound from *Murraya koenigii* (L) Spreng. Drug Des Devel Ther. 2018;12:1119–1133; doi: https://doi.org/10.2147/dddt.s156826
29. Voon FL, Lee YZ, Ooi XY, Tay CZE, Tan JW, Tham CL, et al. Purpurin as a promising anticancer agent: a review of preclinical evidence. Fitoterapia 2026;189:107052; doi: https://doi.org/10.1016/j.fitote.2025.107052
30. Wang YH, Goto M, Wang LT, Hsieh KY, Morris-Natschke SL, Tang GH, *et al.* Multidrug resistance-selective antiproliferative activity of Piper amide alkaloids and synthetic analogues. Bioorg Med Chem Lett 2014;24(20):4818–21; doi: https://doi.org/10.1016/j.bmcl.2014.08.063
31. Barshir R, Fishilevich S, Iny-Stein T, Zelig O, Mazor Y, Guan-Golan Y, *et al.* GeneCaRNA: a comprehensive gene-centric database of human non-coding RNAs in the GeneCards suite. J Mol Biol 2021;433(11):166913; doi: https://doi.org/10.1016/j.jmb.2021.166913
32. Wu Y, Liu X, Li G. Integrated bioinformatics and network pharmacology to identify the therapeutic target and molecular mechanisms of Huangqin decoction on ulcerative Colitis. Sci Rep 2022;12(1):159; doi: https://doi.org/10.1038/s41598-021-03980-8
33. Franceschini A, Szklarczyk D, Frankild S, Kuhn M, Simonovic M, Roth A, *et al.* STRING v9. 1: protein-protein interaction networks, with increased coverage and integration. Nucleic Acids Res 2013;41(D1):D808–D815; doi: https://doi.org/10.1093/nar/gks1094
34. Szklarczyk D, Franceschini A, Wyder S, Forslund K, Heller D, Huerta-Cepas J, *et al.* STRING v10: protein–protein interaction networks, integrated over the tree of life. Nucleic Acids Res 2015;43(1):D447–452; doi: https://doi.org/10.1093/nar/gku1003
35. Flórez AF, Park D, Bhak J, Kim BC, Kuchinsky A, Morris JH, *et al.* Protein network prediction and topological analysis in *Leishmania* major as a tool for drug target selection. BMC Bioinf 2010;11(1):484; doi: https://doi.org/10.1186/1471-2105-11-484
36. Chen L, Chu C, Lu J, Kong X, Huang T, Cai YD. Gene ontology and KEGG pathway enrichment analysis of a drug target-based classification system. PLoS One 2015;10(5):e0126492; doi: https://doi.org/10.1371/journal.pone.0126492

How to cite this article:
Jumana A, Vazhayil J, Harikumar S, Anas A, Poonthiruthi S, Jafar RM. Multi-target modulation of prostate cancer signaling by *Boerhavia diffusa* leaf constituents: Insights from network pharmacology-guided *in silico* and *in vitro* approaches. J Appl Biol Biotech 2026;14(6):119-126. DOI: 10.7324/jabb.2026.316331